IEEE Access
Multidisciplinary | Rapid Review | Open Access Journal

Received December 13, 2019, accepted January 7, 2020, date of publication February 7, 2020, date of current version February 18, 2020.

*Digital Object Identifier 10.1109/ACCESS.2020.2972287*

# Inter-Numerology Interference Management With Adaptive Guards: A Cross-Layer Approach

**ALI FATIH DEMIR[1], (Student Member, IEEE), AND HÜSEYIN ARSLAN[1,2], (Fellow, IEEE)**
[1]Department of Electrical Engineering, University of South Florida, Tampa, FL 33620, USA
[2]Department of Electrical and Electronics Engineering, Istanbul Medipol University, 34810 Istanbul, Turkey

Corresponding author: Ali Fatih Demir (afdemir@mail.usf.edu)

**ABSTRACT** The next-generation communication technologies are evolving towards increased flexibility in various aspects. Although orthogonal frequency division multiplexing (OFDM) remains as the waveform of the upcoming fifth-generation (5G) standard, the new radio provides flexibility in waveform parametrization (a.k.a. numerology) to address diverse requirements. However, managing the peaceful coexistence of mixed numerologies is challenging due to inter-numerology interference (INI). This paper proposes the utilization of adaptive guards in both time and frequency domains as a solution along with a multi-window operation in the physical (PHY) layer. The adaptive windowing operation needs a guard duration to reduce the unwanted emissions, and a guard band is required to handle the INI level on the adjacent band. The guards in both domains are jointly optimized with respect to the subcarrier spacing, use case (i.e., service requirement), and power offset between the numerologies. Also, the multi-window approach provides managing each side of the spectrum independently in case of an asymmetric interference scenario. Since the allowed interference level depends on the numerologies operating in the adjacent bands, the potential of adaptive guards is further increased and exploited with a medium access control (MAC) layer scheduling technique. The proposed INI-based scheduling algorithm decreases the need for guards by allocating the numerologies to the available bands, considering their subcarrier spacing, power level, and SIR requirements. Therefore, INI management is performed with a cross-layer (PHY and MAC) approach in this study. The results show that the precise design that accommodates such flexibility reduces the guards significantly and improves the spectral efficiency of mixed numerology systems.

**INDEX TERMS** 5G, interference management, numerology, OFDM, scheduling, windowing.

## I. INTRODUCTION

The next generation wireless communication technologies are envisioned to support a diverse range of services under the same network. As a recent example, the International Telecommunications Union (ITU) has defined the main use cases that are going to be supported in the fifth generation (5G) mobile network as enhanced mobile broadband (eMBB), massive machine type communications (mMTC), and ultra-reliable low-latency communications (URLLC) [1] as shown in Fig. 1. The applications which demand high data rate and better spectral efficiency fall into the eMBB category, whereas the ones which require ultra-high connection density and low power consumption falls into the mMTC category. Moreover, the mission-critical applications, where errors and retransmissions are less tolerable, are categorized in URLLC. A flexible air interface is needed to meet these demanding service requirements under various channel conditions and system scenarios. Hence, the waveform, which is the main component of any air interface, must be designed precisely to facilitate such flexibility.

Orthogonal frequency-division multiplexing (OFDM) is the most popular waveform that is currently being used in various standards such as 4G LTE and the IEEE 802.11 family [2]. It provides several tempting features such as efficient hardware implementation, low-complexity equalization, and easy multiple-input-multiple-output (MIMO) integration. On the other hand, OFDM seriously suffers from its high out-of-band emissions (OOBE), peak-to-average power ratio (PAPR), and strict synchronization requirements. In addition, 4G LTE adopts a uniform OFDM parameter configuration in pursuit of orthogonality and cannot serve

The associate editor coordinating the review of this manuscript and approving it for publication was Walid Al-Hussaibi.


**FIGURE 1.** 5G use cases: (a) Enhanced mobile broadband, (b) ultra-reliable low-latency communications, and (c) massive machine type communications.

different needs efficiently. Numerous waveforms have been proposed [3]–[7] considering all these disadvantages, but none of them can address all the requirements of the upcoming 5G standard [8]. Therefore, OFDM remains as the waveform of the new radio [9]–[11], and a flexible waveform parametrization, which is also known as numerology [12], [13], is introduced to embrace diverse requirements.

The channel conditions, use cases, and system scenarios are the most critical considerations for the numerology design. For example, the subcarrier spacing of OFDM should be kept large to handle the Doppler spread in a highly mobile environment. On the other hand, a smaller subcarrier spacing provides a longer symbol duration and decreases the relative redundancy that is allocated for time dispersion. An efficient numerology design ensures better utilization of spectral resources and numerology multiplexing will be one of the core technologies in the new radio [14]. However, managing the coexistence of multiple numerologies in the same network is challenging. Although OFDM numerologies are orthogonal in the time domain, any mismatch in parametrization, such as subcarrier spacing, leads to inter-numerology interference (INI) in the frequency domain [12], [15]. Despite the fact that it is a new interference type, which will be an issue for 5G, extensive research led to in-depth INI analyses and various INI management techniques [12], [15]–[22]. For instance, windowing [16], [17] and filtering [18], [20] operations are performed at both transmitter and receiver side along with the guard band allocation to mitigate the unwanted emissions from non-orthogonal numerologies. In addition, it is demonstrated that mixed transparent waveform processing can be applied to optimize the complexity-performance trade-off at transmitter and receiver separately [19]. Precoding techniques at the transmitter [21], [23] and interference cancellation algorithms at the receiver [16] are also considered for multi-numerology coexistence. Last but not least, waveform multiplexing [12], [22] is suggested for mixed numerology management as well. Among these physical (PHY) layer techniques, the windowing operation has a relatively less complexity, which is almost at the same level compared to CP-OFDM [19]. Also, the windowing approach preserves the essential structure of the OFDM transceivers and provides backward compatibility for the current OFDM-based systems. The windowing operation requires an extra period, which extends the guard duration between the consecutive OFDM symbols. Also, additional guard bands are still required between adjacent channels to deal with the INI. In other words, better interference mitigation is realized with the cost of reduced spectral efficiency. Accordingly, the future communication systems have to optimize the guards in both time and frequency domains to improve the spectral efficiency.

This paper proposes the utilization of adaptive guards along with a multi-window operation in the PHY layer to manage the INI, which is an issue in the mixed numerology systems. The guard band and the window parameters that handle the guard duration are jointly optimized regarding the subcarrier spacing, use case, and power offset between the numerologies. Also, the multi-window technique provides managing each side of the spectrum independently in case of an asymmetric interference scenario. Since the allowed interference level depends on the numerologies operating in the adjacent bands, the potential of adaptive guards is further increased and exploited with a medium access control (MAC) layer scheduling technique. The proposed INI-based scheduling algorithm decreases the need for guards by allocating the numerologies to the available bands, considering the subcarrier spacing, power level, and SIR requirements. Therefore, INI management is performed with a cross-layer (PHY and MAC) approach in this study. The preliminary results without a mixed-numerology guard optimization, a multi-window operation, or an elaborate INI-based scheduling algorithm and its evaluation were presented in [24]. Recently, a U.S. patent [25] is issued for the proposed technique as well. The main contributions of this paper are listed as follows:

- The key parameters for guard allocation are identified considering a mixed numerology system.

- The guards in both time and frequency domains are jointly optimized with respect to the subcarrier spacing, use case, and power offset between the numerologies.
- An interference based scheduling algorithm is proposed to decrease the need for guards.

The remaining part of this paper is structured as follows. Section II is dedicated to the system model, and it describes the guard design methodology in detail. Section III presents the guard optimization procedure considering the key parameters of the mixed numerology system. Section IV introduces the INI-based scheduling algorithm along with the utilization of adaptive guards. Finally, Section V summarizes the contributions and concludes the paper.

## II. SYSTEM MODEL

Consider the uplink of a multiuser OFDM system, where asynchronous numerologies with different subcarrier spacing, power level, and use case (i.e., service requirements) operate in the same network. Each numerology can serve multiple synchronous user equipments (UEs) and is assigned to a different bandwidth part (BWP) [10]. A transmitter windowing operation is performed to improve the spectral localization of numerologies and manage interference level on the adjacent BWPs. The guard duration that is allocated for the time-dispersive channel (i.e., $T_{CP-Ch}$) is fixed, and it is adequate to deal with the inter-symbol interference (ISI). Also, an extra guard duration is needed for windowing operation. Various windowing functions have been compared thoroughly [26] with different trade-offs between the main lobe width and the side lobe suppression. The optimal windowing function is outside the scope of this paper, and a raised-cosine (RC) window is utilized due to its low computational complexity and widespread use in the literature [27]–[29]. The RC window function [27] is formulated by the following equation:

$$g[n] = \begin{cases} \frac{1}{2} + \frac{1}{2}\cos\left(\pi + \frac{\pi n}{\alpha N_{\mathrm{T}}}\right) & 0 \le n \le \alpha N_{\mathrm{T}} \\ 1 & \alpha N_{\mathrm{T}} \le n \le N_{\mathrm{T}} \\ \frac{1}{2} + \frac{1}{2}\cos\left(\pi - \frac{\pi n}{\alpha N_{\mathrm{T}}}\right) & N_{\mathrm{T}} \le n \le (\alpha + 1)\, N_{\mathrm{T}}, \end{cases} \tag{1}$$

where $\alpha$ is the roll-off factor ($0 \le \alpha \le 1$) and $N_{\mathrm{T}}$ denotes the symbol length. The roll-off factor ($\alpha$) handles the taper duration of the RC window function. As $\alpha$ increases, the INI decreases with the cost of increased redundancy. The transmitter windowing operation is shown in Fig. 2. Initially, the guard duration is increased with an additional cyclic prefix (CP) and a newly added cyclic suffix (CS). Afterward, the window function is applied to the extended symbol. The transition parts (i.e., ramp-ups and ramp-downs) of adjacent symbols are overlapped to reduce the time-domain overhead emerging from the windowing operation.

Usually, the windowing operation is not enough to manage the inter-numerology interference (INI), and non-negligible

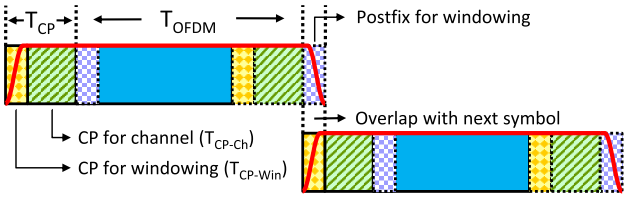


**FIGURE 2.** Transmitter windowing operation and guard duration allocation.

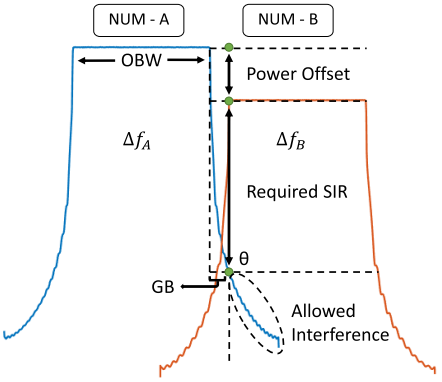


**FIGURE 3.** Guard band allocation between two numerologies considering the allowed interference level ($\theta$) in the adjacent band.

guard bands are still required. However, the total amount of guard band (GB) or the length of guard duration (GD) which is needed for windowing operation depends on the subcarrier spacing of the interference source, the required signal to interference ratio (SIR) level of the numerology in its adjacent bands, and the power offset (PO) between them. The adaptive guard concept is represented with two numerologies in Fig. 3 and can be generalized to multiple numerologies by considering one pair at a time. The threshold for allowed interference level on the adjacent band is represented with $\theta$, and it is expressed as follows:

$$\theta_{\Delta f,i} = P_i - P_j + S_j, \tag{2}$$

where $P_i$ represents the in-band power of the interference source, $S_j$ denotes the required SIR in the adjacent band to achieve a given target bit error rate considering device complexity for processing, and $\Delta f$ indicates the subcarrier spacing of the interference source. It should be noted that the different use case requirements and device capabilities are reflected in the required SIR parameter, power level, and subcarrier spacing. Also, $\theta_{\Delta f}$ implies an adaptive brick-wall type spectral mask for a simple evaluation in this study. However, it is possible to extend it to more complicated mask structures along with the adjacent channel leakage ratio (ACLR) threshold [30]. The guards in both time and frequency domains are utilized regarding $\theta_{\Delta f}$ to achieve the desired SIR level of the numerology on the adjacent band. Throughout the numerical evaluations in this study, GD (i.e., $T_{CP-Win}$) and GB are adaptive, and these guards are optimized in Section III. Also, a multi-window operation [31], [32] can be performed in case

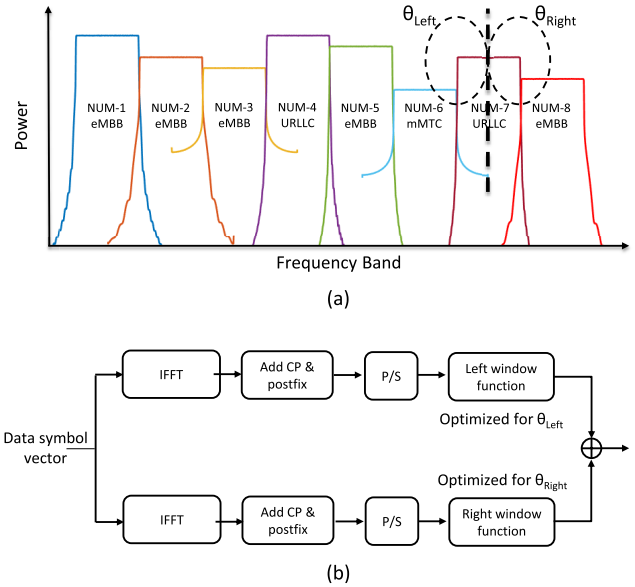


**FIGURE 4.** (a) Asymmetric interference scenario in a mixed numerology network; (b) Block diagram of the multi-window operation.

**TABLE 1.** Simulation parameters.

| Parameter | Value | | | |
|---|---|---|---|---|
| Subcarrier Spacing (kHz) | 15 | 30 | 60 | 120 |
| $T_{OFDM}$ (μs) | 66.7 | 33.3 | 16.7 | 8.3 |
| $T_{CP\text{-}channel}$ (μs) | 4.68 | 2.34 | 1.17 | 0.59 |
| FFT Size | 2048 | | | |
| Number of Active Subcarriers | 1024 | | | |
| $CP_{channel}$ Size | 144 | | | |
| # OFDM Symbols | 300 | | | |
| Window Type | Multi-window | | | |
| Window Function | Raised Cosine | | | |

of an asymmetric interference scenario to manage each side of the spectrum independently considering $\theta_{Left}$ and $\theta_{Right}$ as shown in Fig. 4. The total CP length must be kept the same for synchronicity when a multi-window operation is performed, and the extra CP duration is reserved to solve possible time-domain issues. The remaining parameters of the windowed-OFDM (W-OFDM) system are listed in Table 1.

The potential of adaptive guards is increased further, along with the utilization of INI-based scheduling algorithm. Consider frequency domain multiplexed $M$ asynchronous numerologies as shown in Fig. 5. Different channel conditions, use cases, and system scenarios result in a change in subcarrier spacing, power level, and SIR requirement of the numerologies as mentioned in Section I. The optimal numerology assignment is beyond the scope of this study, and the reader is referred to [33] for more details on this topic. In this article, the spectral efficiency is optimized while ensuring the required SIR levels for a given numerology set. The power level and SIR requirement of each numerology

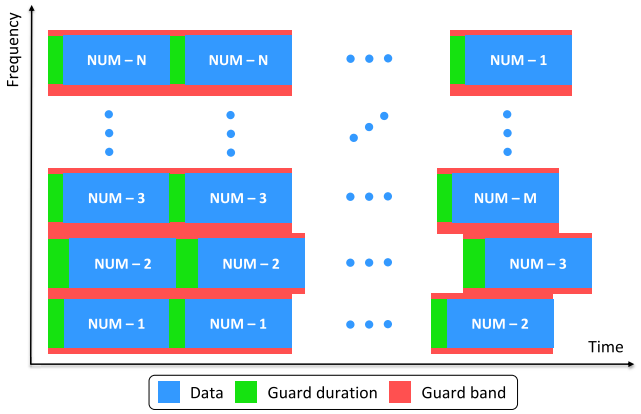


**FIGURE 5.** Frequency domain multiplexed numerologies.

are generated randomly in such a way that $\theta$ changes from 0 dB to 60 dB. Also, $\Delta f$ gets discrete values of {15, 30} kHz and {60, 120} kHz with a uniform probability distribution in the frequency range-1 (FR1, a.k.a. sub-6 GHz bands) and frequency range-2 (FR2, a.k.a. millimeter-wave bands) [9], respectively. Assuming that the base station obtains all these necessary information perfectly and there are $M$ available subbands, it allocates the numerologies to the available subbands out of $M!$ possible arrangements intelligently considering the INI.

## III. OPTIMIZATION OF THE ADAPTIVE GUARDS

Assuming that the data at each subcarrier are statistically independent and mutually orthogonal, the power spectral density (PSD) of an OFDM signal is obtained by summing the power spectra of individual subcarriers, and it is expressed by the following equation [34]–[36]:

$$P_f(x) = \frac{\sigma_d^2}{T} \sum_k |G[(f - k\Delta f)\,T]|^2\,, \tag{3}$$

where $\sigma_d^2$ represents the variance of the data symbols, $T$ denotes the symbol duration, $k$ stands for the subcarrier index, $\Delta f$ shows the subcarrier spacing, and $G$ is the frequency domain representation of pulse shaping window. An OFDM signal is well localized in the time domain with a rectangular pulse shape, which is equivalent to a sinc shape in the frequency domain. The sidelobes of the sincs result in a serious INI issue, and they should be reduced to prevent interference. Particularly, the frequency domain localization is crucial for asynchronous transmissions across adjacent subbands and peaceful coexistence with other numerologies in the network. The sidelobes of RC function is controlled with the parameter $\alpha$ as shown in the following relationship [37]:

$$G = \frac{\sin(\pi fT)}{\pi fT} \frac{\cos(\pi \alpha fT)}{1 - (2\alpha fT)^2} \quad 0 \le \alpha \le 1. \tag{4}$$

Equation 3 and equation 4 show that the parameters $T$ (i.e., $\Delta f = 1/T$) and $\alpha$ have an important effect on the PSD of W-OFDM. Figure 6 illustrates the effect of these parameters

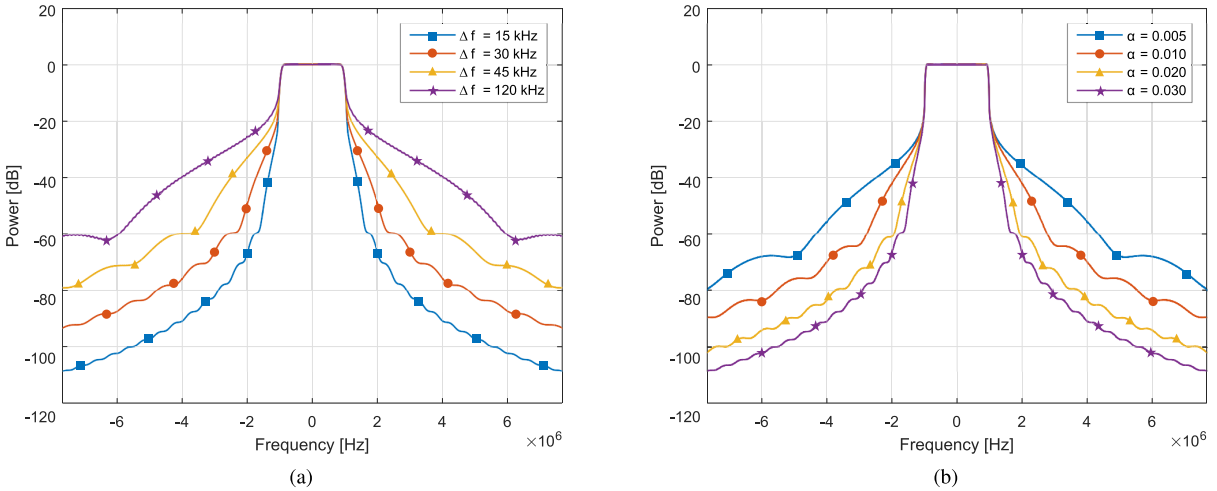


**FIGURE 6.** PSD of W-OFDM: (a) The effect of $\Delta f$ ($\alpha$ is fixed to 0.03); (b) The effect of $\alpha$ ($\Delta f$ is fixed to 15kHz).

on the PSD separately. It should be noted that a significant contribution to unwanted emissions in the passband comes from RF front-end impairments as well, including power amplifier nonlinearities. However, these impairments heavily depend on many implementation-dependent factors, such as the application type, operational frequency, bandwidth of the signal, and complexity of the device, and are not considered in this study.

In a mixed numerology network, the INI can be managed by windowing operation and allocating guard band between adjacent numerologies as described in Section II. Since the windowing operation reduces the unwanted emissions with a cost of extra guard duration, the INI management procedure boil downs to the adaptive utilization of guard duration (GD) and guard band (GB) to achieve a desired interference threshold ($\theta$). Figure 7 demonstrates the required GB and GD amounts for selected $\theta$ values considering a W-OFDM signal with $\Delta f = 15\ kHz$. Each $\alpha$ value in the figure represents a GD allocation to carry out windowing operation, and a GB allocation to handle the rest of interference for a given $\theta$.

A tremendous time-frequency resource is required to deal with the INI issue only with GB or GD allocation. Hence, GB and GD have to be jointly optimized in order to improve the spectral efficiency, which is measured as the information rate that can be transmitted over a given bandwidth. This hyper-parameter optimization has been carried out by a grid search method through a manually designated subset of the hyper-parameter space [38]. The spectral efficiency ($\eta$) is proportional to the multiplication of efficiencies in the time and frequency domains, which are calculated as follows:

$$\eta_{time} = \frac{T_{OFDM}}{T_{OFDM} + T_{CP-Ch} + T_{CP-Win}}, \tag{5}$$

$$\eta_{freq} = \frac{OBW}{OBW + (GB \times 2)}. \tag{6}$$

Considering $T_{OFDM}$, $T_{CP-Ch}$, and occupied bandwidth ($OBW$) are fixed parameters for a given $\Delta f$, the degrees of freedom that can be selected independently becomes only GB and GD (i.e., $T_{CP-Win}$). The optimization problem that looks for the optimal GB and GD pair can be defined as follows:

$$(GB,\ GD) = \arg\max_{GB,\ GD}(\eta_{time} \times \eta_{freq}), \tag{7}$$

$$\text{subject to: } P_i - P_j + S_j \leq \theta_{\Delta f,i}. \tag{8}$$

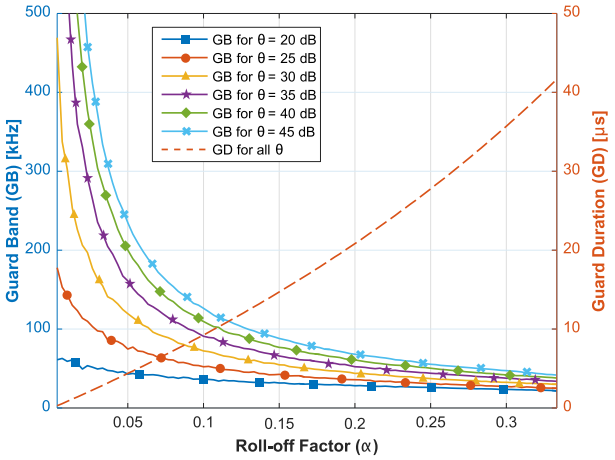


**FIGURE 7.** Required GB and GD pairs to achieve selected $\theta$ levels for a W-OFDM signal with $\Delta f = 15\ kHz$.

The spectral efficiencies for selected $\theta$ values are shown in Fig. 8. Each $\alpha$ value in the figure is equivalent to a GB-GD pair for a given $\theta$, and the peak value of each curve determines the optimal pair. These optimal pairs are summarized in Table 2 along with the related parameters for various $\Delta f$. The results reveal that the need for windowing diminishes as $\theta$ decreases, and accordingly, the desired interference level can be accomplished only with a few guard subcarriers. Also, the spectral efficiency increases with the decrease in $\theta$. The change in required guards clearly confirms that the adaptive guard design enhances the spectral efficiency significantly compared to designing the mixed numerology

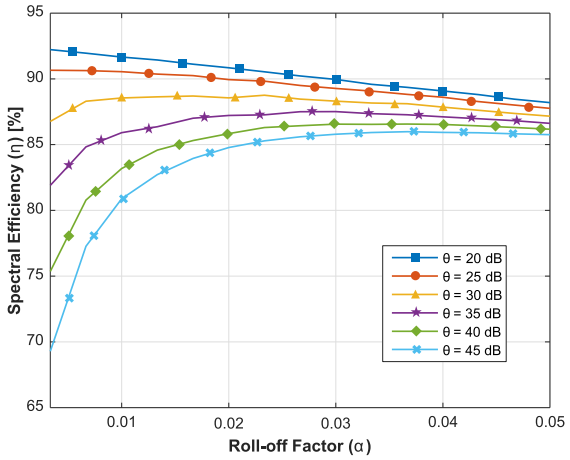


**FIGURE 8.** Spectral efficiency ($\eta$) of the GB and GD pairs that achieves selected $\theta_{\Delta f=15\,kHz}$ (Please note that each $\alpha$ corresponds to a GB-GD pair).

system considering the worst case scenario (e.g., $\eta_{\theta=45\,dB} = 85.98$ % whereas $\eta_{\theta=20\,dB} = 92.53$ %). Despite the fact that the computational complexity increases compared to traditional OFDM-based systems, the computation of the optimal GB-GD pairs is an offline action that needs a one-time calculation. Therefore, a lookup table procedure can be used to decrease complexity.

## IV. INTER-NUMEROLOGY INTERFERENCE (INI)-BASED SCHEDULING

The total guard amount is reduced with the joint optimization of the guard band (GB) and guard duration (GD) for a given interference threshold ($\theta_{\Delta f}$) in Section III. The optimization results show that the spectral efficiency ($\eta$) decreases as $\theta$ increases. Also, the numerologies with larger subcarrier spacing ($\Delta f$) require more guards, and they lead to lower $\eta$ values in a mixed numerology network. Since $\theta$ depends on the numerologies operating in the adjacent bands, the potential of adaptive guards can be enhanced further along with the utilization of an interference-based scheduling algorithm.

The proposed scheduling algorithm groups the numerologies and allocate them to the available subbands considering the inter-numerology interference (INI). The numerologies with similar subcarrier spacing, power level, and SIR requirements are arranged together in order to decrease the mean $\theta$ in the network. Consequently, the need for guards reduces, and the spectral efficiency improves. The steps of the proposed INI-based scheduling algorithm are listed as follows:

1) Sort the numerologies regarding their $\Delta f$ value in an ascending/descending order.
2) Calculate the similarity metric for all numerologies as $\beta_j = SIR_j - P_j$.
3) Sort $\beta$ in an ascending/descending order for the numerologies with the same $\Delta f$.
4) If $\beta$ value repeats, sort based on power in the adjacent band.

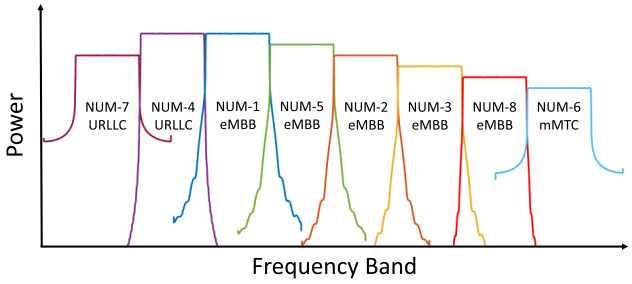


**FIGURE 9.** INI-based scheduled numerologies with various use cases.

5) Check $P$ on both sides of the available band. If $P$ is the same with the numerology in its adjacent band, allocate the numerology with a higher SIR requirement to the edge.

The performance of the INI-based scheduling algorithm is evaluated numerically, and its performance is compared with the performance of a random scheduling strategy. The allocation probability to any given subband is $1/M$ for all numerologies (i.e., uniform probability distribution) in the random scheduling strategy. Eight numerologies (i.e., $M = 8$) are considered in Monte Carlo simulations, and a random parameter set is assigned to numerologies for each realization, as discussed in Section II. The key parameters of an exemplary realization, such as subcarrier spacing, power level, and SIR requirement, are listed in Tables 3 and 4. The random scheduling strategy and the INI-based scheduling strategy are implemented for the same parameter set, as illustrated in Fig. 4 and Fig. 9, respectively. Although the guards in both time and frequency domains are jointly optimized in the PHY layer for both cases, they utilize different scheduling algorithms in the MAC layer. As a result, any performance difference can be attributed to the proposed scheduling algorithm. Furthermore, a fixed guard allocation strategy is implemented with the random scheduling method to demonstrate the effectiveness of the proposed adaptive guard allocation. The guards are assigned considering the worst-case scenario (i.e., highest $\theta_{\Delta f}$) in the fixed guard allocation strategy.

The system performance is evaluated in terms of spectral efficiency ($\eta$) and the average evaluation results (out of 100 independent realizations) for various guard allocation and scheduling strategies, which are the fixed guard allocation with the random scheduling, the adaptive guard allocation with the random scheduling, and the adaptive guard allocation with the INI-based scheduling, are presented in Table 5. The results demonstrate that the GD and GB amounts are reduced by 43% and 34%, respectively when the fixed guards are replaced with the adaptive guards in the frequency range-1 (FR1) scenario. Also, the GD and GB amounts are reduced further by 10% and 27%, respectively, when the proposed INI-based scheduling strategy is implemented instead of the random scheduling strategy. It is worth to note that $\eta$ is lower in the frequency range-2 (FR2) case since more guards are required for the numerologies with higher $\Delta f$ values

**TABLE 2.** Optimal guard duration (GD) and guard band (GB) pairs for selected $\theta$.

| θ [dB] | $\Delta f = 15$ kHz | | | | $\Delta f = 30$ kHz | | | | $\Delta f = 60$ kHz | | | | $\Delta f = 120$ kHz | | | |
|---|---|---|---|---|---|---|---|---|---|---|---|---|---|---|---|---|
| | α | GD [μs] | GB [kHz] | η [%] | α | GD [μs] | GB [kHz] | η [%] | α | GD [μs] | GB [kHz] | η [%] | α | GD [μs] | GB [kHz] | η [%] |
| 20 | 0.0000 | 0.00 | 74.88 | 92.53 | 0.0000 | 0.00 | 154.44 | 92.50 | 0.0000 | 0.00 | 249.83 | 92.68 | 0.0000 | 0.00 | 557.22 | 92.59 |
| 25 | 0.0033 | 0.23 | 210.11 | 90.65 | 0.0033 | 0.11 | 390.13 | 90.83 | 0.0033 | 0.06 | 857.94 | 90.60 | 0.0033 | 0.03 | 1582.9 | 90.79 |
| 30 | 0.0233 | 1.69 | 217.33 | 88.75 | 0.0167 | 0.60 | 534.34 | 88.79 | 0.0167 | 0.30 | 1037.3 | 88.88 | 0.0167 | 0.15 | 2121.9 | 88.81 |
| 35 | 0.0300 | 2.21 | 272.87 | 87.51 | 0.0267 | 0.98 | 609.44 | 87.47 | 0.0300 | 0.55 | 1083.9 | 87.53 | 0.0267 | 0.24 | 2426.1 | 87.49 |
| 40 | 0.0367 | 2.70 | 306.71 | 86.57 | 0.0300 | 1.11 | 715.19 | 86.59 | 0.0333 | 0.62 | 1318.6 | 86.58 | 0.0367 | 0.34 | 2449.7 | 86.57 |
| 45 | 0.0367 | 2.70 | 360.58 | 85.98 | 0.0367 | 1.35 | 722.70 | 85.98 | 0.0367 | 0.68 | 1434.8 | 86.01 | 0.0367 | 0.34 | 2886.1 | 85.98 |

**TABLE 3.** Key parameters of randomly scheduled numerologies for adaptive guard allocation.

| Band | 1 | 2 | 3 | 4 | 5 | 6 | 7 | 8 |
|---|---|---|---|---|---|---|---|---|
| Numerology ID | 1 | 2 | 3 | 4 | 5 | 6 | 7 | 8 |
| Δf [kHz] | 30 | 15 | 15 | 30 | 15 | 15 | 30 | 15 |
| Req. SIR [dB] | 20 | 20 | 20 | 25 | 20 | 25 | 35 | 20 |
| Rx Power [dBm] | 0 | -10 | -15 | 0 | -5 | -25 | -10 | -20 |
| Power Offset [dB] | 10 | -10, 5 | -5, -15 | 15, 5 | -5, 20 | -20, -15 | 15, 10 | -10 |
| Intf. Thr. ($\theta_A$, $\theta_B$) [dB] | 30 | 10, 25 | 15, 10 | 35, 25 | 20, 45 | 0, 20 | 40, 30 | 25 |

**TABLE 4.** Key parameters of INI-based scheduled numerologies for adaptive guard allocation.

| Band | 1 | 2 | 3 | 4 | 5 | 6 | 7 | 8 |
|---|---|---|---|---|---|---|---|---|
| Numerology ID | 7 | 4 | 1 | 5 | 2 | 3 | 8 | 6 |
| Δf [kHz] | 30 | 30 | 30 | 15 | 15 | 15 | 15 | 15 |
| Req. SIR [dB] | 35 | 25 | 20 | 20 | 20 | 20 | 20 | 25 |
| Rx Power [dBm] | -10 | 0 | 0 | -5 | -10 | -15 | -20 | -25 |
| Power Offset [dB] | -10 | 10, 0 | 0, 5 | -5, 5 | -5, 5 | -5, 5 | -5, 5 | -5 |
| Intf. Thr. ($\theta_A$, $\theta_B$) [dB] | 15 | 45, 20 | 25, 25 | 15, 25 | 15, 25 | 15, 25 | 15, 30 | 15 |

**TABLE 5.** Spectral efficiency comparison for various guard allocation and scheduling strategies.

| Scenario | Total Guard Duration [μs] | | Total Guard Band [kHz] | | Spectral Efficiency [%] | |
|---|---|---|---|---|---|---|
| | FR1 | FR2 | FR1 | FR2 | FR1 | FR2 |
| Fixed Guards & Random Scheduling | 16.08 | 4.12 | 5018.4 | 1927.4 | 81.22 | 77.35 |
| Adaptive Guards & Random Scheduling | 9.09 | 2.24 | 3335.7 | 1310.2 | 85.32 | 82.19 |
| Adaptive Guards & INI-based Scheduling | 8.15 | 2.06 | 2428.8 | 971.9 | 87.10 | 84.65 |

due to their higher unwanted emissions. Although it can be compensated with an increased number of subcarriers (FR2 is suitable for wider bands), it is kept as fixed to 256 for a fair comparison with the FR1 case in the numerical evaluations.

The proposed INI-based scheduling strategy is particularly important when there is a severe power imbalance between the numerologies (i.e., a set of synchronous UEs). The current mobile networks adopted a power control mechanism in the uplink to manage interference between neighboring bands. However, this solution restricts the UEs with better channel conditions to deploy higher-order modulations and decreases the spectral efficiency. The proposed scheduling technique can relax the power control mechanism and improve throughput. Also, it should be noted that the channel-based scheduling can be performed to orthogonal/synchronous UEs within a given numerology, whereas the INI-based scheduling can be performed to non-orthogonal/asynchronous numerologies for reduced complexity.

## V. CONCLUSIONS

A novel inter-numerology interference (INI) management technique with a cross-layer approach is proposed in this paper. The adaptive guards in both time and frequency domains are utilized along with a multi-window operation in the PHY layer and jointly optimized considering the use case, subcarrier spacing, and power offset between the numerologies. Since the allowed interference level depends on the numerologies operating in the adjacent bands, the potential of adaptive guards is further increased and exploited with a MAC layer scheduling technique. The proposed INI-based scheduling algorithm decreases the need for guards by allocating the numerologies to the available bands, considering their subcarrier spacing, power level, and SIR requirements. It is demonstrated that the optimized guard allocation and INI-based scheduling algorithm improves the spectral efficiency significantly while taking into account the different use case requirements and device capabilities.

The results show that the precise design that accommodates such flexibility reduces the guards and improves the performance of mixed numerology systems. The INI management technique is proposed on the transmitter side in the PHY layer along with a MAC layer scheduling technique in this study. The guards are designed in such a way that it guarantees the required SIR levels for each numerology in the network. Therefore, the theoretical upper bounds on the bit error rate can be obtained in a straightforward way using the channel capacity equation [39]. However, it will be extended to the receiver side as well for enhanced performance in the future. Also, a practical receiver structure enables performance evaluation under various channel conditions and impairments. Furthermore, the CP length for the multipath channel is assumed fixed and sufficient for the

delay spread. Nevertheless, some ISI can be allowed in order to suppress INI further for a fixed guard duration, and the ISI vs. INI trade-off is worth investigating. Last but not least, the proposed INI management technique with a cross-layer approach can be applied to other spectrally enhanced OFDM systems [40]–[43] as well by optimizing the waveform parameters and guards along with a proper scheduling mechanism. For example, a recent publication [18] demonstrated the joint optimization of the filter parameters and guard band for filtered-OFDM (f-OFDM) only in the PHY layer.

The next-generation wireless communication technologies are evolving towards increased flexibility in various aspects. Enhanced flexibility is the key design consideration, especially to be able to serve diverse requirements. Hence, the adaptive guard utilization must be a part of the future communication systems.

## REFERENCES

[1] *IMT Vision—Framework and Overall Objectives of the Future Development of IMT for 2020 and Beyond*, ITU-R, Geneva, Switzerland, Sep. 2015.

[2] T. Hwang, C. Yang, G. Wu, S. Li, and G. Y. Li, "OFDM and its wireless applications: A survey," *IEEE Trans. Veh. Technol.*, vol. 58, no. 4, pp. 1673–1694, May 2009.

[3] A. F. Demir, M. Elkourdi, M. Ibrahim, and H. Arslan, "Waveform design for 5G and beyond," in *5G Networks: Fundamental Requirements, Enabling Technologies, and Operations Management*. Hoboken, NJ, USA: Wiley, 2018, ch. 2, pp. 51–76.

[4] X. Zhang, L. Chen, J. Qiu, and J. Abdoli, "On the waveform for 5G," *IEEE Commun. Mag.*, vol. 54, no. 11, pp. 74–80, Nov. 2016.

[5] *Waveform Candidates*, document R1-162199, 3GPP, Qualcomm Inc., Busan, South Korea, Apr. 2016.

[6] A. Sahin, R. Yang, E. Bala, M. C. Beluri, and R. L. Olesen, "Flexible DFT-S-OFDM: Solutions and challenges," *IEEE Commun. Mag.*, vol. 54, no. 11, pp. 106–112, Nov. 2016.

[7] G. Berardinelli, K. I. Pedersen, T. B. Sorensen, and P. Mogensen, "Generalized DFT-spread-OFDM as 5G waveform," *IEEE Commun. Mag.*, vol. 54, no. 11, pp. 99–105, Nov. 2016.

[8] H. Huawei, *5GWaveform: Requirements and Design Principles*, document R1-162151, 3GPP, Busan, South Korea, Apr. 2016.

[9] Y. Kim, Y. Kim, J. Oh, H. Ji, J. Yeo, S. Choi, H. Ryu, H. Noh, T. Kim, F. Sun, Y. Wang, Y. Qi, and J. Lee, "New radio (NR) and its evolution toward 5G-advanced," *IEEE Wireless Commun.*, vol. 26, no. 3, pp. 2–7, Jun. 2019.

[10] S. Parkvall, E. Dahlman, A. Furuskar, and M. Frenne, "NR: The new 5G radio access technology," *IEEE Commun. Stand. Mag.*, vol. 1, no. 4, pp. 24–30, Dec. 2017.

[11] S.-Y. Lien, S.-L. Shieh, Y. Huang, B. Su, Y.-L. Hsu, and H.-Y. Wei, "5G new radio: Waveform, frame structure, multiple access, and initial access," *IEEE Commun. Mag.*, vol. 55, no. 6, pp. 64–71, Jun. 2017.

[12] Z. E. Ankarali, B. Pekoz, and H. Arslan, "Flexible radio access beyond 5G: A future projection on waveform, numerology, and frame design principles," *IEEE Access*, vol. 5, pp. 18295–18309, 2017.

[13] A. A. Zaidi, R. Baldemair, H. Tullberg, H. Bjorkegren, L. Sundstrom, J. Medbo, C. Kilinc, and I. Da Silva, "Waveform and numerology to support 5G services and requirements," *IEEE Commun. Mag.*, vol. 54, no. 11, pp. 90–98, Nov. 2016.

[14] H. Huawei, *Scenario and Design Criteria on Flexible Numerologies*, document R1-162156, 3GPP, Busan, South Korea, Apr. 2016.

[15] A. B. Kihero, M. S. J. Solaija, and H. Arslan, "Inter-numerology interference for beyond 5G," *IEEE Access*, vol. 7, pp. 146512–146523, 2019.

[16] X. Zhang, L. Zhang, P. Xiao, D. Ma, J. Wei, and Y. Xin, "Mixed numerologies interference analysis and inter-numerology interference cancellation for windowed OFDM systems," *IEEE Trans. Veh. Technol.*, vol. 67, no. 8, pp. 7047–7061, Aug. 2018.

[17] B. Pekoz, Z. E. Ankarali, S. Kose, and H. Arslan, "Non-redundant OFDM receiver windowing for 5G frames and beyond," *IEEE Trans. Veh. Technol.*, vol. 69, no. 1, pp. 676–684, Jan. 2020.

[18] M. Yang, Y. Chen, and L. Du, "Interference analysis and filter parameters optimization for uplink asynchronous F-OFDM systems," *IEEE Access*, vol. 7, pp. 48356–48370, 2019.

[19] T. Levanen, J. Pirskanen, K. Pajukoski, M. Renfors, and M. Valkama, "Transparent Tx and Rx waveform processing for 5G new radio mobile communications," *IEEE Wireless Commun.*, vol. 26, no. 1, pp. 128–136, Feb. 2019.

[20] J. Yli-Kaakinen, T. Levanen, S. Valkonen, K. Pajukoski, J. Pirskanen, M. Renfors, and M. Valkama, "Efficient fast-convolution-based waveform processing for 5G physical layer," *IEEE J. Sel. Areas Commun.*, vol. 35, no. 6, pp. 1309–1326, Jun. 2017.

[21] L. Zhang, A. Ijaz, P. Xiao, A. Quddus, and R. Tafazolli, "Subband filtered multi-carrier systems for multi-service wireless communications," *IEEE Trans. Wireless Commun.*, vol. 16, no. 3, pp. 1893–1907, Mar. 2017.

[22] Y.-G. Lim, T. Jung, K. S. Kim, C.-B. Chae, and R. A. Valenzuela, "Waveform multiplexing for new radio: Numerology management and 3D evaluation," *IEEE Wireless Commun.*, vol. 25, no. 5, pp. 86–94, Oct. 2018.

[23] Y. Huang and B. Su, "Circularly pulse-shaped precoding for OFDM: A new waveform and its optimization design for 5G new radio," *IEEE Access*, vol. 6, pp. 44129–44146, 2018.

[24] A. F. Demir and H. Arslan, "The impact of adaptive guards for 5G and beyond," in *Proc. IEEE 28th Annu. Int. Symp. Pers., Indoor, Mobile Radio Commun. (PIMRC)*, Oct. 2017, pp. 1–5.

[25] A. F. Demir and H. Arslan, "System and method for adaptive OFDM guards," U.S. Patent 10 411 819, Sep. 2019.

[26] B. Farhang-Boroujeny, "OFDM versus filter bank multicarrier," *IEEE Signal Process. Mag.*, vol. 28, no. 3, pp. 92–112, May 2011.

[27] T. Weiss, J. Hillenbrand, A. Krohn, and F. K. Jondral, "Mutual interference in OFDM-based spectrum pooling systems," in *Proc. IEEE 59th Veh. Technol. Conf.*, vol. 4, May 2004, pp. 1873–1877.

[28] E. Bala, J. Li, and R. Yang, "Shaping spectral leakage: A novel low-complexity transceiver architecture for cognitive radio," *IEEE Veh. Technol. Mag.*, vol. 8, no. 3, pp. 38–46, Sep. 2013.

[29] A. Sahin, I. Guvenc, and H. Arslan, "A survey on multicarrier communications: Prototype filters, lattice structures, and implementation aspects," *IEEE Commun. Surveys Tuts.*, vol. 16, no. 3, pp. 1312–1338, 3rd Quart., 2014.

[30] *New Radio (NR); Base Station (BS) Radio Transmission and Reception*, document TS 38.104 V15.4.0, 3GPP, Technical Specification Group Radio Access Network, Release 15, Dec. 2018.

[31] A. Sahin and H. Arslan, "Edge windowing for OFDM based systems," *IEEE Commun. Lett.*, vol. 15, no. 11, pp. 1208–1211, Nov. 2011.

[32] *Discussion on Multi-Window OFDM for NR Waveform*, document R1-166746, 3GPP, Gothenburg, Sweden, Aug. 2016.

[33] A. Yazar and H. Arslan, "A flexibility metric and optimization methods for mixed numerologies in 5G and beyond," *IEEE Access*, vol. 6, pp. 3755–3764, 2018.

[34] T. Van Waterschoot, V. Le Nir, J. Duplicy, and M. Moonen, "Analytical expressions for the power spectral density of CP-OFDM and ZP-OFDM signals," *IEEE Signal Process. Lett.*, vol. 17, no. 4, pp. 371–374, Apr. 2010.

[35] S. Talbot and B. Farhang-Boroujeny, "Spectral method of blind carrier tracking for OFDM," *IEEE Trans. Signal Process.*, vol. 56, no. 7, pp. 2706–2717, Jul. 2008.

[36] C. Liu and F. Li, "Spectrum modelling of OFDM signals for WLAN," *Electron. Lett.*, vol. 40, no. 22, pp. 1431–1432, Oct. 2004.

[37] L. Montreuil, R. Prodan, and T. Kolze, "OFDM TX symbol shaping," in *Proc. IEEE P802.3bn EPoC Interim Meeting*, Phoenix, AZ, USA, Jan. 2013. Accessed: Feb. 10, 2020. [Online]. Available: http://www.ieee802.org/3/bn/public/jan13/montreuil_01a_0113.pdf

[38] J. S. Bergstra, R. Bardenet, Y. Bengio, and B. Kégl, "Algorithms for hyper-parameter optimization," in *Proc. Adv. Neural Inf. Process Syst.*, 2011, pp. 2546–2554.

[39] J. G. Proakis, *Digital Communications*. New York, NY, USA: McGraw-Hill, 2001.

[40] X. Zhang, M. Jia, L. Chen, J. Ma, and J. Qiu, "Filtered-OFDM-enabler for flexible waveform in the 5th generation cellular networks," in *Proc. IEEE Global Commun. Conf. (GLOBECOM)*, Dec. 2014, pp. 1–6.

[41] V. Vakilian, T. Wild, F. Schaich, S. T. Brink, and J.-F. Frigon, "Universal-filtered multi-carrier technique for wireless systems beyond LTE," in *Proc. IEEE Globecom Workshops (GC Wkshps)*, Dec. 2013, pp. 223–228.

[42] G. Fettweis, M. Krondorf, and S. Bittner, "GFDM-generalized frequency division multiplexing," in *Proc. IEEE 69th Veh. Technol. Conf. (VTC Spring)*, Apr. 2009, pp. 1–4.

[43] B. Farhang-Boroujeny and H. Moradi, "OFDM inspired waveforms for 5G," *IEEE Commun. Surveys Tuts.*, vol. 18, no. 4, pp. 2474–2492, May 2016.

**ALI FATIH DEMIR** (Student Member, IEEE) received the B.S. degree in electrical engineering from Yıldız Technical University, Istanbul, Turkey, in 2011, and the M.S. degree in electrical engineering and applied statistics from Syracuse University, Syracuse, NY, USA, in 2013. He is currently pursuing the Ph.D. degree, as a member of the Wireless Communication and Signal Processing (WCSP) Group, at the Department of Electrical Engineering, University of South Florida, Tampa, FL, USA. His current research interests include PHY and MAC aspects of wireless communication systems, wireless body area networks (WBANs), and signal processing/machine learning algorithms for brain–computer interfaces (BCIs).

**HÜSEYIN ARSLAN** (Fellow, IEEE) received the B.S. degree in electrical and electronics engineering from Middle East Technical University, Ankara, Turkey, in 1992, and the M.S. and Ph.D. degrees in electrical engineering from Southern Methodist University, Dallas, TX, USA, in 1994 and 1998, respectively. From January 1998 to August 2002, he was with the Research Group, Ericsson Inc., Charlotte, NC, USA, where he was involved with several projects related to 2G and 3G wireless communication systems. Since August 2002, he has been with the Department of Electrical Engineering, University of South Florida, Tampa, FL, USA, where he is currently a Professor. In December 2013, he joined Istanbul Medipol University, Istanbul, Turkey, where he has worked as the Dean of the School of Engineering and Natural Sciences. His current research interests include waveform design for 5G and beyond, physical layer security, dynamic spectrum access, cognitive radio, coexistence issues on heterogeneous networks, aeronautical (high altitude platform) communications, and *in vivo* channel modeling and system design. He is currently a member of the Editorial Board of the *Sensors Journal* and the IEEE COMMUNICATIONS SURVEYS AND TUTORIALS.